Vortex dynamics and their interactions in quantum trajectories

D A Wisniacki[1], **E R Pujals**[2] **and F Borondo**[3]

[1] Departamento de Física "J. J. Giambiagi", FCEN, UBA, Pabellón 1, Ciudad Universitaria, 1428 Buenos Aires, Argentina
[2] IMPA–OS, Dona Castorina 110, 22460–320, Rio de Janeiro, Brazil
[3] Departamento de Química C–IX, Universidad Autónoma de Madrid, Cantoblanco, 28049 Madrid, Spain

E-mail: wisniacki@df.uba.ar, enrique@impa.br and f.borondo@uam.es

Abstract

Vortices are known to play a key role in many important processes in physics and chemistry. Here, we study vortices in connection with the quantum trajectories that can be defined in the framework provided by the de Broglie–Bohm formalism of quantum mechanics. In a previous work, it was shown that the presence of a single moving vortex is enough to induce chaos in these trajectories. Here, this situation is explored in more detail by discussing the relationship between Lyapunov exponents and the parameters characterizing the vortex dynamics. We also consider the issue when more than one vortex exists. In this case, the interaction among them can annihilate or create pairs of vortices with opposite vorticity. This phenomenon is analyzed from a dynamical point of view, showing how the size of the regular regions in phase space grows, as vortices disappear.

PACS numbers: 03.65.+w, 03.65.Ta

1. Introduction

Bohmian mechanics (BM) was originally introduced in the 1950s [1] as an alternative formulation of quantum mechanics, with the aim of solving some of the fundamental interpretational difficulties existing in the standard version [2]. Past this initial period, and with a more computationally oriented view, it has experienced recently an important revitalization, having become at present a powerful tool for the study of many interesting physical processes [3]. The perspective used in BM, which is based on quantum trajectories (QT) piloted by the system's de Broglie wave [4] (see section 2 below), combines both the predictive accuracy of

the quantum theory with the capability of providing intuitive interpretations of the underlying physical phenomena [5], and represents a true theory of quantum motion [6].

The nature of BM makes the consideration of the dynamical characteristics of QTs a crucial point in this theory. Unfortunately, this issue has been ignored very often in the literature, or treated from a very naive or even wrong point of view. Frisk [7] has pointed out towards a possible relationship existing between vortices and chaos in QTs. Very recently, the authors have made what we consider a relevant advance along this line in [8, 9], which has also contributed to place the problem on firm grounds. In these two papers, the importance of the vortices of the associated velocity field was shown, also establishing the functional relationship existing between their dynamics and the complexity or ergodicity [10] of the QTs. In particular, our work has clearly shown that QTs are, in general, intrinsically chaotic, and the very restrictive conditions in which this is not so were also discussed.

Vortices have attracted a great deal of attention and interest in many scientific fields since early times in physics. They are associated to singularities at which the corresponding mathematical magnitudes become infinity or change abruptly, and are now widely recognized as an interesting subject of study *per se* [11]. In classical physics, vortices are known to play a prominent role in fluid dynamics [12], meteorology [13], particle trapping in planetesimal and star formation [14], liquid crystals [15], oscillatory reaction [16], combustion and flames [17], non-linear optics [18], and more recently in the growing business of microfluidics [19]. They are also important quantum mechanically, being central to superfluidity [20], superconductivity [21], wave-guides [22], long-distance electron tunneling in biomolecules [23], chemical reaction dynamics [5, 24] and very recently in connection with Bose–Einstein condensation [25]. Vortitial motions are highly relevant in nonlinear quantum dynamics, since they mediate the corresponding stability and interactions among vortices, something that has been shown very important in BEC condensates [26] and optics [27].

The chaotic properties of QTs have been recently shown to be critical in relation to a cornerstone in the interpretation of quantum mechanics as it is Born's probability rule: $\rho = |\psi|^2$. This relation still remains a postulate after a century of quantum physics, although it has been revisited in the last years by several authors [28–30] in order to make probability an emergent phenomenon [31]. The most important work in relation to the interests of the present paper is that of Valentini and Westman [30]. These authors numerically explored an speculation contained in the original papers by Bohm, according to which probabilities have a dynamical origin, and behave similarly to thermal probabilities in ordinary statistical mechanics [32]. These calculations showed how the standard distribution is obtained as the time evolution towards equilibrium of initial non-equilibrium states, $\rho \neq |\psi|^2$, this taking place with an exponential decrease in the associated coarse-grained *H*-function. Although not explicitly mentioned by the authors, ergodicity of QTs is required to support their arguments. In this respect, the typicality of $|\psi|^2$ at equilibrium has also been discussed in the literature [33].

In this paper, we extend our previous work [8, 9] to the role played by vortices as an active agent to induce complexity in QTs. For this purpose, we study the quantum dynamics in a simple system (2D harmonic oscillator) for which the classical counterpart is integrable, considering an increasing number of these vortitial singularities. For the case of a single vortex, we have developed and analyzed the results of a simplified model, in which the dynamics of the QTs is assumed to be exclusively determined by the influence of the existing vortex. The computational efficiency of this model is high, since it allows a very fast calculation of the main dynamical characteristics of the associated QTs and its relation to the vortex motion, which is otherwise very time consuming even for the simplest physical models. For more than one vortex, we concentrate our study on the dynamical consequences of the

corresponding annihilation and/or creation processes, that have been shown by us to be a key factor controlling QT chaoticity. When pair of vortices disappear, temporarily or otherwise, sizeable parts of configuration space in which QTs evolve regularly are created, and this effect is enough to decrease their complexity. Concurrently, the opposite effect takes place when vortices appear, and the balance between these two counteracting tendencies and its evolution in time completely determines global chaoticity of a given system.

The organization of this paper is as follows. In the next section we briefly review the theory in which our calculations are based, and the models that have been used. In particular, the fundamental equations in the de Broglie–Bohm formalism of quantum mechanics, the so-called quantum trajectories, and how vortices appear in the theory are briefly described. Also, we discuss in this section the fundamental role played by vortices in relation to the main point addressed in this work, i.e. the chaoticity and complexity of the QTs. Finally, section 4 is devoted to the presentation of our results, and the paper concludes with a summary of the main conclusions.

2. Bohmian mechanics, vortices and chaos

The QT–BM formalism starts from the suggestion made by Madelung [34] of writing the wavefunction in a polar form

$$\psi(r, t) = R(\mathbf{r}, t) \exp[iS(\mathbf{r}, t)], \tag{1}$$

where $R = \psi^*\psi$ and $S = (\ln \psi - \ln \psi^*)/(2i)$ ($\hbar$ is set equal to unity throughout the paper) are two real functions of position and time. Substitution of this expression into the time-dependent Schrödinger equation allows to recast quantum theory into a 'hydrodynamical' form, governed by:

$$\frac{\partial R^2}{\partial t} + \nabla \cdot \left(R^2 \frac{\nabla S}{m} \right) = 0, \qquad \frac{\partial S}{\partial t} + \frac{(\nabla S)^2}{2m} + V + Q = 0, \tag{2}$$

which are the continuity and 'quantum' Hamilton–Jacobi (HJ) equations, respectively. The qualifying term 'quantum' applies to the last equation due the fact that it contains an extra term with respect to the usual HJ equation [35]. This non-local term, determined by the quantum state and given by

$$Q = \frac{1}{2m} \frac{\nabla^2 R}{R}, \tag{3}$$

is usually called 'quantum potential'. Together with V, it determines the total force acting on the system. Actually, this extra contribution is responsible for introducing the (eventual) quantum effects into the dynamics of the system.

Similarly to what happens in the standard HJ theory [35], equations (2) allow us to introduce, for spinless particles, 'quantum trajectories' for the system. These QTs are obtained by integration of the following differential equation:

$$\mathbf{v} = \dot{\mathbf{r}} = \frac{\nabla S}{m} = \frac{i}{2m} \frac{\psi \nabla \psi^* - \psi^* \nabla \psi}{|\psi|^2}, \tag{4}$$

defining the corresponding velocity field.

According to the probabilistic interpretation of quantum mechanics, QTs are the paths along which the probability flows in the quantum fluid. The quantum state is therefore defined, in this interpretation of quantum mechanics, by $\psi(\mathbf{r}, t)$ and $\mathbf{r}(t)$, that evolve simultaneously in a deterministic way, in which the pilot wave ψ guides the particles, each one starting at a different position [4, 6].

Due to its 'hydrodynamical' nature, vortices appear quite naturally in BM. From the mathematical point of view, these vortices are related to the regions in which the wavefunction, ψ, vanishes, and they are the result of the wavefunction interferences. In this sense, they have a purely quantum nature, with no corresponding classical explanation. In the absence of magnetic fields, the bulk vorticity, $\nabla \times \mathbf{v}$, in the quantum probability fluid is determined by the points where the phase, S, is singular. This happens at isolated points for 2D systems and in lines for the 3D case. The condition leading to the formation of quantum vortices [36] arises from the complex character of the wavefunction and its single-valuedness condition, that lead to the condition

$$S'(\mathbf{r}, t) = S(\mathbf{r}, t) + 2\pi n, \qquad n = 0, \pm 1, \pm 2, \ldots, \tag{5}$$

implying that the circulation, Γ, along any closed contour, $\mathcal{C}$, encircling a vortex must be quantized [37] according to

$$\Gamma = m \oint_{\mathcal{C}} \dot{\mathbf{r}} \cdot d\mathbf{r} = \oint_{\mathcal{C}} \nabla S \cdot d\mathbf{r} = 2\pi n. \tag{6}$$

From this condition, it follows that the velocity $\mathbf{v}$ must diverge as one approaches the vortex position. Actually, the time-dependent velocity field in the vicinity of a vortex located at the time t at $\mathbf{r}_v(t)$ is given to first order by [38, 39]

$$v = -\frac{i}{2m} \frac{[\mathbf{r} - \mathbf{r}_v(t)] \times (\mathbf{w} \times \mathbf{w}^*)}{|[\mathbf{r} - \mathbf{r}_v(t)] \cdot \mathbf{w}|^2}. \tag{7}$$

where $\mathbf{w} \equiv \nabla \psi(\mathbf{r}_v(t))$. Since quantum vortices have zero thickness, this approximation is always valid sufficiently close to the vortex. Actually, an estimation of the relative error as well as second-order expressions can be found in [39]. Moreover, equation (7) exactly fulfills the quantization condition (6), something that reinforces its reliability.

In a previous paper [8], it was shown that vortices play a fundamental role in the dynamical character of QTs. In particular, the existence of a single moving vortex is enough to induce chaotic dynamics in the QTs. What happens here is that the motion of the vortex produces a saddle point, with stable and unstable manifolds that exhibit topological transverse intersections which generate an homoclinic tangle. On the contrary, when the vortex is still, or fulfill special conditions, these manifolds joined smoothly and the associated QTs describe trajectories which are regular, as can be ascertained with the standard tools of nonlinear dynamics [10].

3. Models

The system that we choose to study is the two-dimensional isotropic harmonic oscillator of unit mass and angular frequency $\omega = 1$. The corresponding Hamiltonian is then given by

$$\hat{H} = -\frac{1}{2} \left(\frac{\partial^2}{\partial x^2} + \frac{\partial^2}{\partial x^2} \right) + \frac{1}{2}(x^2 + y^2). \tag{8}$$

The associated eigenenergies are $E_{n_x, n_y} = n_x + n_y + 1$, and the eigenfunctions can be expressed as

$$\phi_{n_x, n_y}(x, y) = \frac{1}{(\pi 2^{n_x + n_y} n_x! n_y!)^{1/2}} H_{n_x}(x) H_{n_y}(y) \exp\left[-\frac{1}{2}(x^2 + y^2) \right], \quad n_x, n_y = 0, 1, \ldots, \tag{9}$$

where H_n are the nth degree Hermite polynomials.

The main reason for choosing this system is that the physical forces (term V in (2)) are very simple, with the corresponding dynamics being completely regular. In this way, we guarantee that all signs of chaotic behavior that can be found in our calculations are solely due to the effect of the quantum potential Q in (2).

In order to rationalize our results, we will also consider in this paper a simplified model extracted from [8]. The idea is to find the simplest related model that has only the influence of a single vortex. Since it is known that the velocity field in the vicinity of such a point is given by equation (7), we will extend this expression to all configurational space, also imposing the extra simplifying constrains that $w_x = i w_y$ and the vortex trajectory is time-periodic. Under these assumptions, the non-autonomous velocity field is then given by

$$
\begin{aligned}
v_x &= -\frac{y - y_v(t)}{[x - x_v(t)]^2 + [y - y_v(t)]^2}, \\
v_y &= \frac{x - x_v(t)}{[x - x_v(t)]^2 + [y - y_v(t)]^2},
\end{aligned}
\tag{10}
$$

where we will consider the trajectories corresponding to a particle of unit mass. Defining new variables in polar coordinates $\bar{x} = x - x_v(t) = r \cos\theta$ and $\bar{y} = y - y_v(t) = r \sin\theta$, the above expressions result in

$$
\begin{aligned}
v_r &= r[y_v(t) \sin\theta + x_v(t) \cos\theta], \\
v_\theta &= \frac{1}{r} + y_v(t) \cos\theta + x_v(t) \sin\theta.
\end{aligned}
\tag{11}
$$

This non-autonomous velocity field can be interpreted as a perturbation of the autonomous field: $\mathbf{v}_0 = (0, 1/r)$ with the time-periodic term

$$
\mathbf{G}(r, \theta, t) = (r[y_v(t) \sin\theta + x_v(t) \cos\theta], [y_v(t) \cos\theta + x_v(t) \sin\theta])
\tag{12}
$$

The corresponding flow can also be expressed in Hamiltonian form as

$$
H(r, \theta, t) = \frac{\log r}{2} + r[y_v(t) \cos\theta - x_v(t) \sin\theta]).
\tag{13}
$$

Let us finally remark that from this expression it can be easily shown that in this simplified model there is no chaos in the QTs when the motion of the vortex is circular, due to the fact that for this case $H(r, \theta, t) = f(r, \theta + t)$.

4. Results

Our results will be presented in this section, which is divided for convenience into two parts.

In the first one, results for the case with a single vortex are reported. The aim is to extend the study presented in [8] in order to obtain a deeper understanding of the relationship existing between chaos and QTs. This is done by exploring the role played by the mechanical characteristics governing the motion of the vortex, a point that has not been addressed previously.

In the second part, we analyze results for the situation in which a few interacting vortices, annihilating and creating in pairs, exist. The purpose of our research here is to disentangle the relationship existing between vortex interaction and the QT chaoticity degree.

4.1. Single vortex

In [8] it was shown that the motion of vortices implies chaos in the associated QTs. This is observed, for example, if one considers an initial state with a wavefunction given by the
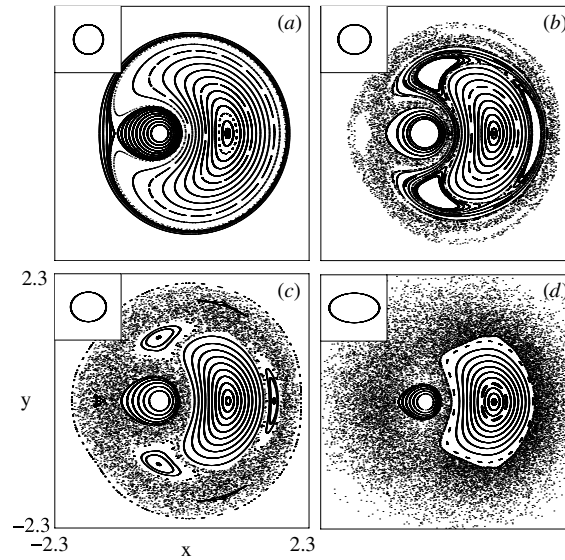
Figure 1. Stroboscopic Poincaré surface of section for the quantum trajectories corresponding to the initial wavefunction given in (14) for values of parameters a and b equal to (a) 0.80, 0.80; (b) 0.80, 0.88; (c) 0.80, 0.96; and (d) 0.80, 1.36. Each plot contains the data from 30 trajectories propagated for 1500 crossings with the surface of section. The trajectory described by the vortex has also been included in the insets.

following combination of eigenstates:

$$\psi_0(x, y) = A\phi_{00} + B\phi_{10} - iC\phi_{01}, \tag{14}$$

where A, B and C are real constants fulfilling the (normalization) condition: $A^2 + B^2 + C^2 = 1$. This wavefunction generates a time-dependent velocity field which has only one vortex, whose trajectories can be obtained analytically as

$$\mathbf{r}_v(t) = (x_v(t), y_v(t)) = \left(-\frac{\sqrt{2}A}{B}\cos t, \frac{\sqrt{2}A}{C}\sin t\right), \tag{15}$$

expression which corresponds to the equation of an ellipse with x and y axes of length $a = \sqrt{2}A/B$ and $b = \sqrt{2}A/C$, respectively.

To ascertain the complexity of the associated QTs, we will use the ideas and tools of nonlinear mechanics [10]; in particular we resort to the use of stroboscopic surfaces of section (SOS) for their visualization. In our case, the non-autonomous velocity field generated by (14) and determination of the QTs is periodic. Accordingly, these trajectories can be suitably monitored by using a stroboscopic SOS defined using the corresponding value of the period, $\omega = 2\pi/(E_{10} - E_{00})$. This SOS is computed by plotting the particle position, (x, y), at fixed values of time given by $t = 2\pi n$, with $n = 0, 1, \dots$. Some results are shown in figure 1.

When the vortex does not move and its position remains fixed (at $(x_v, y_v) = (0, 0)$), the Poincaré SOS consists of concentric circumferences, showing that the motion of the associated QTs is not chaotic. Due to its simplicity, this case is not shown in figure 1. Also, when the vortex moves circularly ($a = b$) the dynamics of the QTs is also regular, but in this case a pitchfork bifurcation of the central fixed point takes place [40], and two new stable fixed points
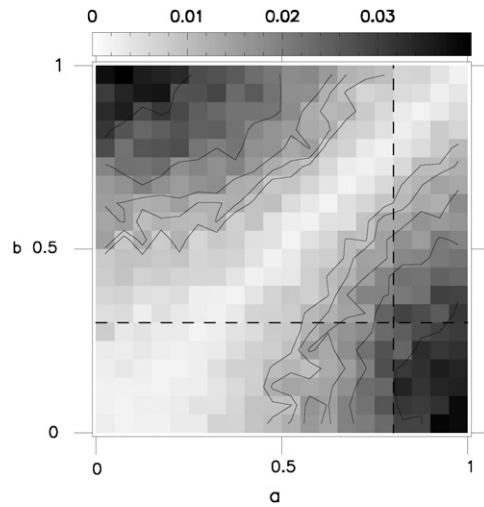
Figure 2. Averaged Lyapunov exponents for the quantum trajectories generated from the simplified model described in section 3, as a function of parameters a and b, corresponding to the lengths of the x and y axes of the elliptic trajectory described by the vortex generated by wavefunction (14).

appear in addition to the old one that becomes unstable. This situation can be seen in panel (*a*) of figure 1.

On the other hand, when the value of a/b increases, and the vortex moves elliptically, a clear transition to chaos takes place and sizeable portions of irregular motion are evident even at small deviations of this parameter from unity (see panels (*b*)–(*d*) in figure 1). Moreover, the fraction of the phase space occupied by these chaotic regions monotonically increases with the value of the eccentricity, a/b. What happens here is that the motion of the vortex produces a saddle point, with stable and unstable manifolds that exhibit topological transverse intersections which generates an homoclinic tangle, organizing the structure of a chaotic band [41]. The existence of this effect, which is not present in the case with $a/b = 1$ shown in panel (a) where the corresponding manifolds joined smoothly, has been rigorously proved in [8]. Some indications on how to construct a (local) approximation explaining the bifurcation giving rise to the saddle point can be found in [40].

A point that still remains open after the work presented in [8] is that concerning the relationship existing between the parameter characteristics of the motion of the vortex and the global chaoticity of the QTs.

To gauge the dynamical complexity of our system we calculate, as it is customary in chaos theory, the Lyapunov exponent of the QTs, λ, statistically averaged over 50 initial conditions randomly distributed in the square $x, y \in [-2, 2]$. A positive value of λ indicates the presence of chaotic behavior, while when $\lambda = 0$ we are in the presence of a completely regular dynamics.

The results for λ, computed from the simplified model described in section 3 for the vortex generated by wavefunction (14) as a function of the parameters a and b (see (15)), are shown in figure 2, in the form of a contours plot. (Note that the wavefunction (14) plays no other role in the calculations of our simplified model but specifying the vortex trajectory, and do not actually intervene in the integration of the simplified QTs.) As can be seen, the results are symmetrical with respect to the diagonal $a = b$, where λ exactly vanishes, the vortex
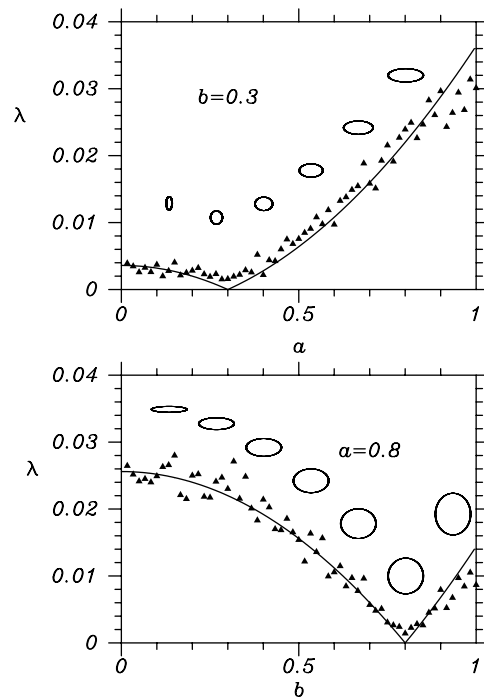
Figure 3. Averaged Lyapunov exponents for the quantum trajectories generated from the simplified model described in section 3, for constant values of the lengths of the y and x axes corresponding to $b = 0.3$ and $a = 0.8$, respectively (filled triangles). A fitting of the results to the parabolic expression $\lambda = 0.04|a^2 - b^2|$ is also shown as a full line. The shapes of the associated vortex trajectories have also been included.

trajectory is circular and the QTs are nonchaotic. This result is not unexpected, since specular points at different sides of the diagonal correspond to a mere change from oblate to prolate configurations (or viceversa), without changing the shape of the vortex trajectory. Clearly, this modification does not affect the character of the associated QTs, as discussed in the previous section. Moreover, figure 2 shows that the averaged Lyapunov exponent grows as we separate from the diagonal, going into regions with larger differences, in absolute value, between a and b. This behavior can be easily rationalized, since by doing this we move away from the regions in which the vortex moves circularly, into more eccentric trajectories; thus implying more chaos in the QTs, as discussed above.

What is more interesting is to analyze in detail this growing behavior. This can be done by analyzing different cuts in the previous plot. Figure 3 shows two such plots: one with the variation of λ along the variable a for a fixed value of $b = 0.3$, and the other with the variation along variable b for $a = 0.8$. The positions of these two cuts have been indicated with dashed lines in figure 2. As can be seen, in both plots the averaged Lyapunov exponent grows with the eccentricity of the ellipse described by the vortex of the velocity field, which have also been plotted in the figure in order that the value of the eccentricity can be visually ascertained. But more interestingly, we find in this figure that λ follows extremely accurately a parabolic, $\lambda \propto |a^2 - b^2|$, law along these two cuts.

To close this subsection, it is interesting to compare the results for the simplified model presented in figures 2 and 3 with those rendered by the full model, in which the QTs are
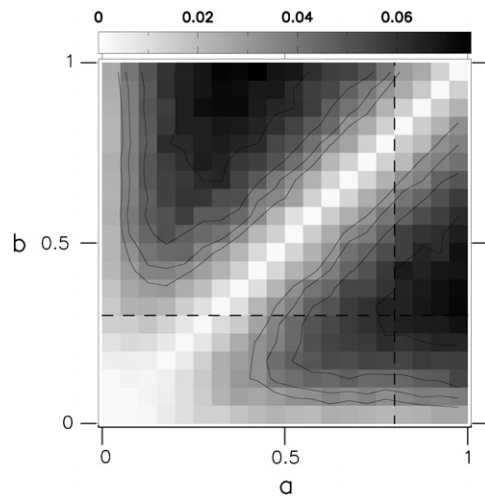
Figure 4. Averaged Lyapunov exponents for the quantum trajectories generated from the initial wavefunction given by (14) (full model described in section 3), as a function of parameters $a = \sqrt{2}A/B$ and $b = \sqrt{2}A/C$, corresponding to the lengths of the axis of the elliptic trajectory described by the associated vortex.
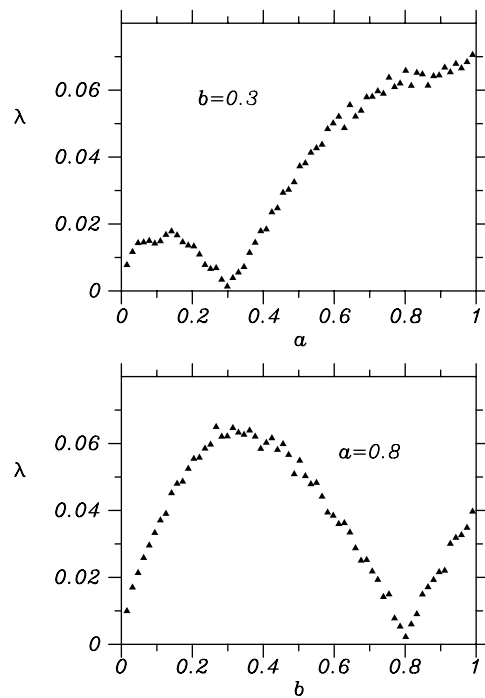

Figure 5. Averaged Lyapunov exponents of the quantum trajectories generated from the initial wavefunction given by (14) and the full model described in section 3, for constant values of the lengths of the y and x-axis corresponding to $b = 0.3$ and $a = 0.8$, respectively.

actually computed from the quantum potential derived from wavefunction (14). The results of the corresponding calculations are shown in figures 4 and 5. As can be seen, the resulting averaged Lyapunov exponents obtained from both models are quite similar, but some important differences exist. In the first place, λ gets here very small (possibly zero) at the axes, $a = 0$ and $b = 0$. The fact that the results obtained in these two calculations are different at the axis is not surprising, and comes from the assumption that $w_x = i w_y$ in the simplified model. This equality would approximately correspond in our case to having coefficients B and C in equation (14) fulfilling condition $B^{-1} = C^{-1}$. The range of values for a and b considered in figures 2 and 4 do not separate significantly from this, except close to both axis, and here is where the results of the approximate (figure 2) and realistic (figure 4) models differ the most. Another point worth discussing is why λ vanishes at the axis. The reason for this is not obvious, but can be understood if one analyzes the situation carefully. For one thing, at the axes we have a vortex describing very eccentric elliptical motions, with trajectories close to a straight line passing through the origin. Accordingly, and as discussed above in connection with the results of figure 1, one should expect a large degree of chaoticity in the corresponding QTs, contrary to the actual findings in the results for λ in figure 4. However, we have here another important counteracting effect. Indeed, when the vortex moves in such eccentric ellipses, it spends a large fraction of time in configurations for which the corresponding quantum density probability is very small, with the net result that the contribution of these very eccentric vortex trajectories in the value of the global chaoticity is negligible, and λ finally gets extremely small.

The corresponding cuts for $b = 0.3$ and $a = 0.8$, depicted in figure 5, also show this behavior. Apart from this difference, when comparing the results in this figure with those for the simplified model shown in figure 3, it is observed that λ is in general larger in the former case than in the latter; consider for example the maxima at $a \simeq 0.14$ in the upper plot and at $b \simeq 0.34$ in the lower one, or the values at $a, b = 1$ in both of them. In physical terms, this result implies that the QTs are, in general, more chaotic in the full model than in the simplified one.

One final interesting comment concerns the asymptotic behavior of the averaged Lyapunov exponent. Although not visible with the scale limits chosen in figures 4 and 5, this parameter goes to zero as either $a, b \to \infty$. Again, and as discussed for the case of the value of λ at the axes, this behavior is the result of two opposite effects. In the first place, we have that for large values of a or b the vortex is orbiting in a loop located very far from the origin, far from the parameter range corresponding to still or circular vortices and thus inducing chaos in the QTs. However, the weight corresponding to these asymptotic regions is negligible and the influence of this vortex in λ is not important.

4.2. Vortex interaction: creation and annihilation

Let us consider now what happens when vortices interact, giving rise to annihilation and/or creation. Remember that when this happens vortices appear or disappear in pairs, each of them with opposite signs of the corresponding vorticity.

The simplest initial wavefunction for which this phenomenon takes place in our case is the following combination of eigenstates:

$$\psi_0'(x, y) = A'\phi_{00} + B'\phi_{20} - iC'\phi_{02}, \tag{16}$$

where A', B' and C' are real constants fulfilling the (normalization) condition: $A'^2 + B'^2 + C'^2 = 1$. This wavefunction has (at most) four vortices, symmetrically located in
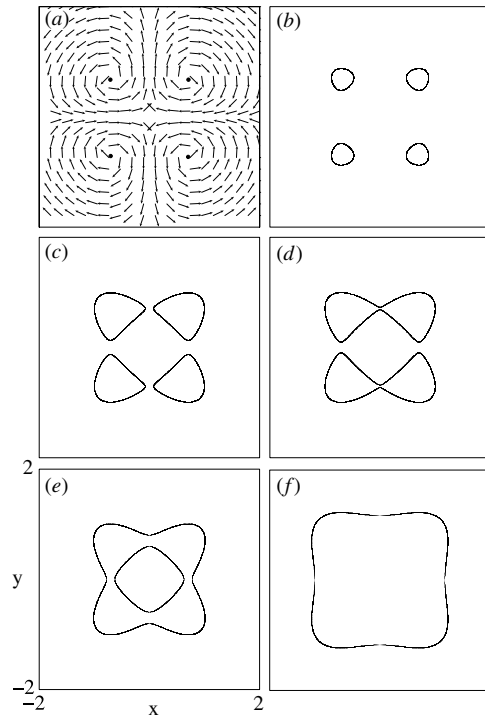
Figure 6. Paths described by the velocity field vortices generated by the initial wavefunction given by (16) with values of the parameters A' and B' equal to (a) 0, 0.6996; (b) 0.2621, 0.6751; (c) 0.4393, 0.6285; (d) 0.4442, 0.6268; (e) 0.4586, 0.6217; and (f) 0.7136, 0.4901. To give an idea of the vorticity corresponding to each vortex, the associated velocity field has been plotted superimposed in panel (a).

the four $x - y$ quadrants, whose positions as a function of time are given by:

$$\mathbf{r}_v(t) = (x_v(t), y_v(t))$$

$$= \left(\pm\sqrt{\frac{1}{2} - \frac{A'}{\sqrt{2}B'} \sin\left(2t + \frac{\pi}{2}\right)}, \pm\sqrt{\frac{1}{2} + \frac{A'}{\sqrt{2}C'} \sin(2t)} \right). \tag{17}$$

According to this expression several quite different situations, as a function of the values given to parameters A', B' and C', can take place. A full account of the most interesting possibilities is summarized in the plots of figure 6.

As can be seen in figure 6(a), for $A' = 0$ the four vortices do not move, being stationary at positions $(\pm 1/\sqrt{2}, \pm 1/\sqrt{2})$, respectively. To give an idea of the vorticity corresponding to each vortex, the associated velocity field has also been plotted superimposed in the figure. As can be observed, contiguous vortices have opposite signs of the vorticity.

As the value of parameter A' increases (thus decreasing the values of both B' and C'), the situation changes and the four vortices acquire some motion, following (17). Some representative trajectories are shown in the other panels of figure 6, where it can be observed that several qualitatively different behaviors exist.

For small enough values of A', the vortices move in trajectories that correspond to closed loop figures which never touch each other, as shown in figure 6(b). In this case, vortices do not annihilate at any time.
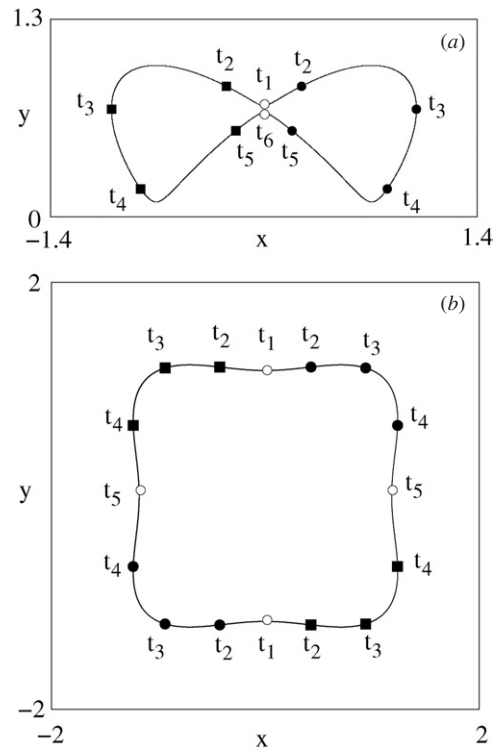
Figure 7. (*a*) Position of the vortices along the trajectory corresponding to: (*a*) Upper loop of figure 6(*d*) at different values of time: $t_{1-6} = 0.03, 0.25, 1.57, 2.20, 2.95, 3.11$. (*b*) Loop of figure 6(*f*) for $t_{1-5} = 0.53, 0.63, 0.97, 1.60$ and 1.83. Vortices annihilate and reappear at points marked with hollow symbols.

As A' further increases, the trajectory loops grow in size (see for example, figure 6(*c*)), eventually getting to the point in which some of them touch each other. When this happens, the two implied vortices annihilate, both disappearing when they simultaneously arrive at the point of contact. The resulting effect is the formation of two symmetrical eight-shaped figures. Past this point, the two loops merge, opening a gap in the region next to the point in which they first made contact. This situation is seen in figure 6(*d*). Now, the vortex dynamics is very interesting, and it is more clearly illustrated in figure 7. In it, the position of the two vortices along the trajectory at increasing values of time has been marked (with full squares for the left vortex and full circles for the right one). If we consider a complete cycle ($T = \pi$), the dynamics go as follows. Let us start at a point just passed t_1. The two vortices then evolve, one clockwise (towards the right) and the other one anticlockwise (towards the left), passing through all the different points marked in the figure at times $t_2 - t_5$, respectively. Afterwards, they then get at the point labeled t_6 on the vertical axis, where the two vortices meet and mutually annihilate. When this happens, they both disappear for a short interval of time, given in our case by $\Delta t = \pi + t_1 - t_6 = 2t_1 = 0.07$, after which they reappear again at the point labeled t_1 (also on the vertical axis). After that the cycle repeats again, with the four vortices going around their respective sections of the whole circuit.

For bigger values of A', the loops described by the vortices touch also at a second point, this taking place now on the horizontal axis. When this happens, a second gap opens, and
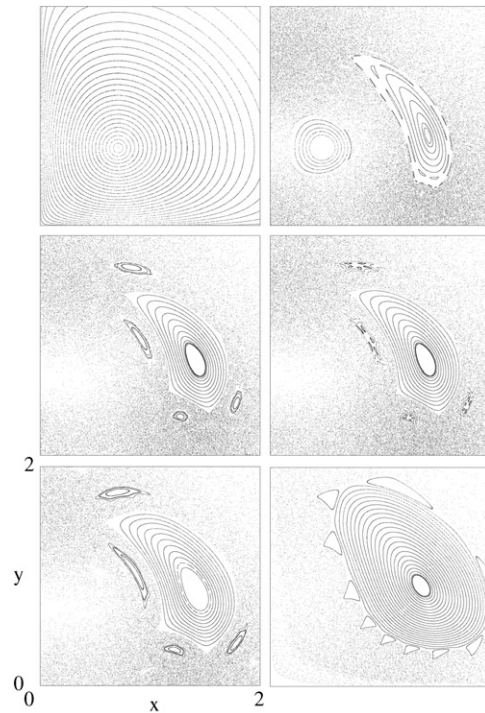
Figure 8. Stroboscopic Poincaré surface of section for the quantum trajectories corresponding to the initial wavefunction given by (16) for the same values of the parameters A' and B' used in figure 6. Due to the symmetry of the figure only the first quadrant has been plotted. Each plot contains the data from 30 trajectories propagated for 3000 crossings with the surface of section.

then we have two closed paths, instead of four, along which the four vortices move in cycles. This situation is shown in figure 6(e). During this motion, the vortices annihilate and are created again periodically, every time that a pair meets either at the vertical or the horizontal axis.

Finally, this pattern continues as A' increases, with the outer path expanding and the inner one shrinking, until a point in which the inner loop disappears. This happens for the largest value of A' considered in this work, and it is shown in figure 6(f). Here the dynamics are similar, with a typical situation in which four vortices, one in each quadrant, exist, as shown in figure 7(b). However, the four of them annihilate simultaneously at t_5, reappearing later at t_1 after and elapsed time interval of $\Delta t = 1.84$, during which no vortices exist.

Let us now consider how this interaction between vortices, implying the creation and annihilation of pairs, affects the global chaoticity of the associated QTs. To gauge this effect, we present in figure 8 some results corresponding to the stroboscopic Poincaré SOS (defined similarly as in figure 1) for the QTs calculated using the initial wavefunction given by (16) for the same values of the parameters A' and B' used in figure 6. As can be seen, the QTs in the first panel are completely regular, as expected since they correspond to a value of $A' = 0$ associated to still vortices. The corresponding trajectories describe in the SOS some sort of triangularly distorted circles around the fixed points located at $(x, y) = (\pm 1/\sqrt{2}, \pm 1/\sqrt{2})$. Note that due to the symmetry of the figure, only the first quadrant has been plotted. As A' increases,

some of the invariant tori in the plot are destroyed due to the perturbation induced by the motion of the vortices and signatures of chaoticity appear in a substantial part of the displayed phase space. However, two relevant islands of regularity still remain. One around the original fixed point $(x, y) = (\pm 1/\sqrt{2}, \pm 1/\sqrt{2})$ and the other around new fixed point located at higher values of $|x|$. In the third panel the regularity islands around $(x, y) = (\pm 1/\sqrt{2}, \pm 1/\sqrt{2})$ disappear, while the others continue their evolution dictated by the Kolmogorov–Arnold– Moser (KAM) theorem [10], for example, a conspicuous chain of islands corresponding to a 1:4 secondary resonance is apparent in the plot. Finally, as A' further increases (last three panels), this latter regularity island grows in size, thus incrementing the fraction of regular QTs.

This non-monotonic behavior, in which the area corresponding to regular QTs first decreases and then increases with A', can be easily explained with the aid of the results shown in figure 6. The plots in this figure clearly show that as A starts increasing (from zero) the motions described by the four existing vortices get more complicated (less circular), thus inducing a more chaotic character in the dynamics of the associated QTs. However, after a certain value of A' (third panel in figure 6), the trajectories of these vortices collide with other at some point, this implying the corresponding annihilation of vortices and later reappearance of them. During these intervals of time, there are regions in configuration space free from vortices, and then the regular character in the dynamics of the QTs is fostered. When considered closely, this is the effect observed in the results of figure 8, where the fraction of regular motion decreases in the first four panels and later increases in the last two.

The behavior that we have just described is also observed in the case in which many vortices exists, as discussed by us in [9], where the estimates of the global chaoticity were assessed statistically. In this way, the study that we are presenting here constitutes the final piece in the puzzle of understanding the relationship existing between chaoticity of QTs in BM and the dynamical characteristics of the associated vortices, and it contributes to fill the gap between the results presented in our two previous works reported in [8, 9], respectively.

5. Summary and conclusions

Summarizing, in this paper we present a theoretical study on the relationship existing between chaos in the QTs appearing in the Bohmian formulation of quantum mechanics and the dynamical characteristics of the motion of the vortices associated to the corresponding velocity field, which is complementary to our previous contributions on this issue [8, 9]. Using a novel simplified model, which takes into account only the influence of a single vortex in the QTs, we have thoroughly analyzed how a given moving vortex induces chaos, quantified through the Lyapunov exponent, in the QTs. Moreover, we have also analyzed the case with few vortices. Here, a new phenomenon, namely the annihilation and later reappearance of pairs of vortices with opposite signs in the vorticity, can takes place. When this happens, portions of the configuration space gets free from vortices and the associated induced chaos in the QTs, which turn accordingly more regular, disappears.

Finally, let us remark that studies such as the one we are presenting here are very important in the recently revitalized topics of BM, since the QTs in which this theory is based are inherently chaotic due to quantum effects. This mean that they may show chaos even in the case in which this phenomenon is not induced by nonlinearities due to the physical potential acting of the system.

Acknowledgments

References

[1] Bohm D 1952 *Phys. Rev.* **85** 166
    Bohm D 1952 *Phys. Rev.* **85** 194
[2] von Neumann J 1955 *Mathematical Foundations of Quantum Mechanics* (Princeton: Princeton University Press)
[3] Philippidis C, Dewdney C and Hiley B J 1979 *Nuovo Cimento Soc. Ital. Fis.* B **52** 15
    Lopreore C L and Wyatt R E 1999 *Phys Rev. Lett.* **82** 5190
    Palao J P, Muga J G and Leavens C R 1999 *Phys. Lett.* A **253** 21
    Prezhdo O V and Brooksby C 2001 *Phys. Rev. Lett.* **86** 3215
    Sanz A, Borondo F and Miret–Artes S 2001 *Europhys. Lett.* **55** 303
    Dürr D, Goldstein S, Tumulka R and Zanghì N 2004 *Phys. Rev. Lett.* **93** 090402
    Oriols X 2007 *Phys Rev. Lett.* **98** 066803
[4] de Broglie L 1926 *Compt. Rend.* **183** 447
[5] Wyatt R E 2005 *Quantum Dynamics with Trajectories: Introduction to Quantum Hydrodynamics* (New York: Springer)
[6] Holland P R 1993 *The Quantum Theory of Motion* (Cambridge: Cambridge University Press)
[7] Frisk H 1997 *Phys. Lett* A **227** 139
[8] Wisniacki D A and Pujals E R 2005 *Europhys. Lett.* **71** 159
[9] Wisniacki D A, Pujals E R and Borondo F 2006 *Europhys. Lett.* **73** 671
[10] Lichtenberg A J and Lieberman M A 2008 *Regular and Chaotic Dynamics* (New York: Springer)
[11] Berry M V 2000 *Nature* **403** 21
[12] Saffman P G 1992 *Vortex Dynamics* (Cambridge: Cambridge University Press)
[13] Davies–Jones R, Trapp R J and Bluestein H B 2001 *Severe Convective Storms* ed C A Doswell, American Meteorological Monograph vol 28 no. 50 pp 167–254 (Boston: American Meteorological Society)
[14] Tanga P, Michel P and Richardson D C 2002 *Astron. Astrophys.* **395** 613
[15] Pismen L M 1999 *Vortices in Nonlinear Fields: From Liquid Crystals to Superfluids; From Non-equilibrium Patterns to Cosmic Strings* (Oxford: Clarendon)
[16] Vinson M, Mironov S, Mulvey S and Pertsov A 1997 *Nature* **386** 477
    Ginn B T and Steinbock O 2004 *Phys. Rev. Lett.* **93** 158301
[17] Poinsot T J and Veynante D P 2004 *Encyclopedia of Computational Mechanics* ed E Stein, R de Borst and T J R Hughes (New York: Wiley)
[18] Desyatnikov A S, Torner L and Kisvshar Y S 2005 *Progress in Optics* vol 47, ed E Wolf
[19] Ottino J M and Wiggins S 2004 *Science* **305** 485
[20] Donnelly R J 1991 *Quantized Vortices in Helium–II* (Cambridge: Cambridge University Press)
[21] Tiley D R and Tiley J 1990 *Superfluidity and Superconductivity* (Bristol: Hilger)
[22] Bromley M W J and Esry B D 2004 *Phys. Rev.* A **70** 013605
[23] Stuchebrukhov A 2003 *Theor. Chem. Acc.* **110** 291
[24] McCullough E A and Wyatt R E 1971 *J. Chem. Phys.* **54** 3578
[25] Matthews M R, Anderson B P, Haljan P C, Wieman C E and Cornell E A 1999 *Phys. Rev. Lett.* **83** 2498
    Dalfovo F, Giorgini S, Pitaevskii L P and Stringari S 1999 *Rev. Mod. Phys.* **71** 463
[26] García–Ripoll J and Pérez–García V M 2000 *Phys. Rev. Lett.* **84** 4264
    García–Ripoll J, Molina–Terriza G, Pérez–García V M and Torner L 2001 *Phys. Rev. Lett.* **87** 140403
[27] Molina–Terriza G, Recolons J, Torres J P, Torner L and Wright E M 2001 *Phys. Rev. Lett.* **87** 023902
[28] Zurek W H 2003 *Phys. Rev. Lett.* **90** 120404
    Zurek W H 2003 *Rev. Mod. Phys.* **75** 716
    Zurek W H 2005 *Phys. Rev.* A **71** 0521105
    See also: Schlosshauer M and Fine A 2005 *Found. Phys.* **35** 197
[29] Wallace D 2003 *Preprint* quant–phy/0312157
    Deutsch D 1999 *Proc. R. Soc. Lond.* A **455** 3129
[30] Valentini A and Westman H 2005 *Proc. R. Soc.* A **461** 253

[31] Adler S L 2004 *Quantum Theory as an Emergent Phenomenon* (Cambridge: Cambridge University Press)
[32] Metiu H 2006 *Statistical Mechanics* (London: Taylor and Francis)
[33] Dürr D, Goldstein S and Zanghi N 1992 *J. Stat. Phys.* **67** 843
[34] Madelung E 1926 *Z. Phys.* **40** 332
[35] Goldstein H, Poole C P and Safko J L 2002 *Classical Mechanics* (Reading, MA: Addison-Wesley)
[36] Dirac P A M 1931 *Proc. R. Soc. Lond.* A **133** 60
[37] Bialynicki–Birula I and Bialynicki–Birula Z 1971 *Phys. Rev.* D **3** 2410
[38] Bialynicki–Birula I, Bialynicki–Birula Z and Sliwa C 2000 *Phys. Rev.* A **61** 032110
[39] Falsaperla P and Fonte G 2003 *Phys. Lett.* A **316** 382
[40] Broer H, Hanssmann H, Jorba A, Villanueva J and Wagener F 2003 *Nonlinearity* **16** 1751
[41] Palis J and Takens F 1993 *Hyperbolicity and Sensitive Chaotic Dynamics at Homoclinic Bifurcations* (Cambridge: Cambridge University Press)